Water Air Soil Pollut (2017) 228: 24
DOI 10.1007/s11270-016-3208-1

Adsorption of Ni(II), Pb(II) and Zn(II) on $Ca(NO_3)_2$-Neutralised Red Mud

Beatriz Cestaro Pichinelli · Mariana Scicia Gabriel da Silva · Fabiano Tomazini da Conceição · Amauri Antonio Menegário · Maria Lucia Pereira Antunes · Guillermo Rafael Beltran Navarro · Rodrigo Braga Moruzzi

Received: 21 July 2016 / Accepted: 6 December 2016 / Published online: 14 December 2016

Abstract This study aimed to investigate a novel method of red mud neutralisation by $Ca(NO_3)_2$ (NRM), keeping its adsorption capacity in relation to natural red mud (RM) for Ni(II), Pb(II) and Zn(II). Results pointed out that the neutralisation process decreases the pH and electrical conductivity values on NRM due to reaction between the carbonate and bicarbonate alkalinity of red mud and calcium from calcium nitrate to form calcite ($CaCO_3$). The maximum adsorption capacity values of RM and NRM, respectively, were 1.78 and 1.79 mmol g^{-1} for Ni(II), 2.13 and 2.23 mmol g^{-1} for Pb(II) and 1.14 and 1.06 mmol g^{-1} for Zn(II). Pseudo-second-order model is the main responsible for the adsorption of these metals on RM and NRM. The adsorption reaction is endothermic and these metals have affinity to RM and NRM. Thus, it is possible to neutralise the red mud with $Ca(NO_3)_2$ without adsorption capacity losses of Ni(II), Pb(II) and Zn(II).

Keywords $Ca(NO_3)_2$-neutralised red mud · Trace metals · Adsorption · Environmental management

B. C. Pichinelli · M. S. G. da Silva
UNESP—Universidade Estadual Paulista, Faculdade de Engenharia de Bauru, Rio Claro, Brazil

F. T. da Conceição (✉) · G. R. B. Navarro · R. B. Moruzzi
UNESP—Universidade Estadual Paulista, Instituto de Geociências e Ciências Exatas, Avenida 24-A, n° 1515, C. P. 178, CEP 13506-900, Bela Vista, Rio Claro, São Paulo, Brazil
e-mail: ftomazini@rc.unesp.br

A. A. Menegário
UNESP—Universidade Estadual Paulista, Centro de Estudos Ambientais, Rio Claro, Brazil

M. L. P. Antunes
UNESP—Universidade Estadual Paulista, Instituto de Ciência e Tecnologia, Rio Claro, Brazil

1 Introduction

Brazil is the third-largest producer of aluminium, making Brazil a contributor to global aluminium production (Brasil 2014). The world bauxite reserves totalled 25.6 billion tonnes in 2013, with the mineable Brazilian bauxite reserves of 714 million tonnes, being produced in 2013 approximately 33 million tonnes, behind Australia and China (Santana 2014). About 95% of the world bauxite production is used in production of alumina (Al_2O_3), which is subjected to an electrolytic reduction, removing oxygen and producing aluminium metal (Mártires 2012).

During the process of alumina extraction from bauxite by Bayer process, it is generated an insoluble waste called red mud (Hind et al. 1999). The amount of generated red mud can reach twice the amount of alumina produced, requiring a large area for disposal. Brazilian red mud presents high alkaline content and is composed primarily of fine particles of SiO_2, Al, Fe, Ca and Ti oxides and hydroxides (Antunes et al. 2012). Disposal methods result in high costs and environmental risks for the aluminium industry. Improper disposal of red mud may lead to problems such as contamination of soil, groundwater and surface water by NaOH, iron,

aluminium or others chemical agents and damage to flora and fauna in the region around the disposal (Hind et al. 1999; Silva Filho et al. 2007).

Neutralisation is a method to minimise the potential environmental impacts caused by red mud disposal or make the red mud reutilisation possible. Neutralisation treatments include water washing (Apak et al. 1998a, b; Cengeloglu et al. 2006; Smiciklas et al. 2014), boiling with acids (Apak et al. 1998a, b; Cengeloglu et al. 2006), washing with acids (Santona et al. 2006; Nadaroglu et al. 2010; Grudić et al. 2013; Liang et al. 2014), and treatment by CO_2 (Sahu et al. 2011) and seawater (McConchie et al. 2000; Palmer et al. 2010; Grudić et al. 2013; Souza et al. 2013a). Calcium nitrate ($Ca(NO_3)_2$) is water soluble and frequently used to extract the exchangeable phase in the desorption of Cd, Pb and Zn from red mud (Santona et al. 2006; Costa et al. 2009). Surprisingly, the use of $Ca(NO_3)_2$ to neutralise red mud has not been previously proposed.

Studies indicated that red mud has substantial adsorptive properties, especially when it receives some type of thermal or chemical treatment (Wang et al. 2008). Besides, red mud is considered a low-cost adsorbent, which can be used in water and wastewater treatment for removal of toxic trace metals (Nadaroglu et al. 2010; Smiljanic et al. 2010; Sahu et al. 2011; Geyikçi et al. 2012; Pulford et al. 2012; Grudić et al. 2013; Smiciklas et al. 2014; Conceição et al. 2016), arsenic (Akin et al. 2012), fluoride (Liang et al. 2014), dyes (Fu et al. 2010; Ratnamala et al. 2012; Souza et al. 2013a, b) and bacteria (Rai et al. 2012).

Trace metals such as lead (Pb), nickel (Ni) and zinc (Zn) are used in various industrial activities such as electroplating and production of alloys, batteries, paints, pigments, dyes and electronic components. These metals are pollutants not compatible with biological treatments. Various technologies have been used to remove trace metals during the water and industrial wastewater treatment, i.e. ion exchange, reverse osmosis, chemical precipitation and adsorption (Tchobanoglous et al. 2003).

Thus, the aims of this study were to investigate a novel method of red mud neutralisation by $Ca(NO_3)_2$ and evaluate its capacity to adsorb Ni(II), Pb(II) and Zn(II), comparing with adsorption capacity of natural red mud. Natural red mud samples were treated with $Ca(NO_3)_2$ and then both materials, RM and $Ca(NO_3)_2$-neutralised red mud (NRM), were characterised in terms of mineralogy, pH, specific surface area, electrical conductivity, specific surface area, chemical and mineralogical composition. The pH influence, adsorption isotherms, kinetics and thermodynamics parameters were studied to better understand Ni(II), Pb(II) and Zn(II) adsorption characteristics in aqueous solutions using natural red mud and $Ca(NO_3)_2$-neutralised red mud.

2 Theoretical Background

2.1 Adsorption Isotherms and Kinetic Studies

Equations used to describe the adsorption isotherms were developed by Freundlich (Eq. 1) and Langmuir (Eq. 2) (Tchobanoglous et al. 2003; Di Bernardo 2005).

$$q_e = K_F C_e^{1/n} \tag{1}$$

$$q_e = \frac{q_{\max} K_L C_e}{1 + K_L C_e} \tag{2}$$

where

K_F = Freundlich capacity factor ((mmol g^{-1})(L $mmol^{-1}$)$^{1/n}$); $1/n$ = Freundlich intensity parameter; q_{max} = maximum amount of adsorption corresponding to complete monolayer coverage on the surface (mmol g^{-1}); K_L = Langmuir constant related to the energy of adsorption (25 mL $mmol^{-1}$).

Models of pseudo-first order Lagergren (Eq. 3), pseudo-second order (Eq. 4), Elovich (Eq. 5) and intraparticle diffusion (Eq. 6) were applied to explain the reaction kinetics and analyse the control mechanism of the adsorption process (Ho and Mckay 1998; Cheung et al. 2000; Önal 2006).

$$\frac{dq_t}{dt} = k_1(q_e - q_t) \tag{3}$$

$$\frac{dq_t}{dt} = k_2(q_e - q_t)^2 \tag{4}$$

$$\frac{dq_t}{dt} = \alpha\, e^{-\beta q_t} \tag{5}$$

$$q_t = k_{int}\, t^{0,5} + C \tag{6}$$

where

q_t and q_e = amount adsorbed at equilibrium (mmol g^{-1}) and at any time t (min); k_1 and k_2 = rate constant of pseudo-first-order rate (min^{-1}) and pseudo-second-order adsorption (g. $mmol^{-1}$ min^{-1}); α = initial sorption rate (mmol g^{-1} min^{-1}); β = extent of surface coverage and activation energy for chemisorption (g $mmol^{-1}$); k_{int} = constant intraparticle diffusion (mmol $g^{-0,5}$ $min^{-0,5}$); C = intercept (mmol $.g^{-1}$).

2.2 Thermodynamic Studies

The thermodynamic study is able to verify the nature of the adsorption reactions, endothermic or exothermic. The variation of standard free energy or Gibbs energy ($\Delta G°$) in J mol^{-1} was calculated from Eq. 7 (Önal 2006). The k_c value was obtained by Eq. 8.

$$\Delta G^\circ = -R.T.\ln K_c \tag{7}$$

$$k_c = \frac{C_{Ae}}{Ce} \tag{8}$$

where:

R = gas constant (J mol^{-1} K^{-1}); k_c = equilibrium constant; T = temperature (K); C_{Ae} and C_e: equilibrium concentration of adsorbate on the adsorbent and in the solution (mmol mL^{-1}), respectively.

The enthalpy change ($\Delta H°$) in J mol^{-1} and the entropy ($\Delta S°$) in J mol^{-1} K^{-1} adsorption were obtained from van't Hoff equation (Eq. 9) (Önal 2006).

$$ln\, k_c = -\frac{\Delta H^\circ}{R\,.\,T} + \frac{\Delta S^\circ}{R} \tag{9}$$

where

$-\Delta H°/R$ = slope of the van't Hoff chart; $\Delta S°/R$ = intercept of the van't Hoff chart.

2.3 Average Relative Error

The average relative error (*ARE*), together with R^2, was chosen to analyse the best-fitting in the isotherm models and kinetic studies to the experimental data, after non-linear adjustment. The *ARE* values were calculated by Eq. 10, adapted from Behnamfard et al. (2014). These values can be positives or negatives, what indicates they were underestimated or overestimated, respectively, compared to the experimental data. Smallest *ARE* absolute values indicate in average more accurate estimation of q_e values, because the calculated value is closer to the experimental value. Selecting the smallest *ARE* absolute values, it was possible to decide which model best represented the adsorption and kinetics of the metals by RM and NRM.

$$\mathrm{ARE} = \frac{100}{N}\sum_{i=1}^{N}\left(\frac{q_{e\ \exp} - q_{e\ \mathrm{cal}}}{q_{e\ \exp}}\right)_i \tag{10}$$

where:

$q_{e\ exp}$ = experimental amount of metal adsorbed onto RM and NRM (mmol g^{-1}); $q_{e\ cal}$ = calculated amount of metal adsorbed onto RM and NRM (mmol g^{-1}); N = number of measurements made.

3 Materials and Methods

3.1 Sampling, Activation Procedures and Characterisation

The red mud used in this study was collected in an aluminium plant in São Paulo State. Natural red mud samples (RM) were defragmented in porcelain crucibles, dried for 12 h at 60 °C and sieved to <150 μm. Samples of neutralised red mud were prepared by washing with an aqueous solution of $Ca(NO_3)_2$ 0.1 N for 2 h at the ratio 1:25 (*wt*/*wt*) of red mud/$Ca(NO_3)_2$ solution. After treatment, the $Ca(NO_3)_2$-neutralised red mud (NRM) was washed with distilled water and dried for 12 h at 60 °C.

The pH and electrical conductivity (EC) values for RM and NRM were determined in 1:25 ratio of red mud/distilled water, using a YSI 556 meter. The combined electrode was calibrated using the following high purity standards at pH 4.00 (4.00 ± 0.01 at 25 °C ± 0.2 °C) and 7.00 (7.00 ± 0.01 at 25 °C ± 0.2 °C). The conductivity metre was calibrated using a 1.0 mmol L^{-1} KCl solution, which corresponds to 147 μS cm^{-1} at 25 °C. The determination of cation exchange capacity (CEC), in $mmol_{(+)}$ kg^{-1}, was performed according to the procedure of Embrapa (1997). The specific surface area (S_{BET}) was characterised by BET/N_2 adsorption methods using a Micromeritics ASAP 2020 instrument. The RM and NRM samples were analysed for SiO_2, Al_2O_3, Fe_2O_{3t}, TiO_2, K_2O, Na_2O, MgO, MnO, CaO, P_2O_5 and LOI (loss on ignition at 1000 °C) by X-ray fluorescence (XRF—Phillips PW 2510). The identification of

minerals was performed by X-ray diffractometry (XRD—Siemens D5000) on powdered samples, using a wide angle X-ray diffractometer, operating at 40 kV and 40 mA, with CuKα radiation. In addition, the morphology of RM and NRM samples was observed under a JEOL JSM-6010LA Scanning Electron Microscope (SEM), attached with an energy dispersive X-ray spectrometer (EDS).

3.2 Adsorption Studies

The Ni(II), Pb(II) and Zn(II) adsorption experiments were conducted using RM and NRM as adsorbents at Environmental Geochemistry Laboratory—IGCE, UNESP, Rio Claro. The solutions of these trace metals have been obtained from their analytical grade nitrate salts : $Ni(NO_3)_2.6H_2O$, $Pb(NO_3)_2$ and $Zn(NO_3)_2.6H_2O$. The influence of pH on the adsorption experiments have been studied at pH values of 2.0, 4.0, 7.0, 10.0 and 12.0. For the experiments with Ni(II), Pb(II) and Zn(II), 1.00 g (±0.01 g) of RM and NRM was mixed to the metal solution at concentration of 1 mmol 25 mL^{-1}. The samples were stirred for 5 h at 145 rpm and the pH control was made with HCl and NaOH, 0.1 M.

Isothermal studies were promoted by contact of 1.00 g (±0.01 g) of adsorbent and 25 mL of Ni(II), Pb(II) or Zn(II) solutions with initial concentrations ranging from 0.5 mmol 25 mL^{-1} to 4.0 mmol 25 mL^{-1} at pH 5.0–5.5. The system was stirred at 145 rpm, for 24 h, at temperature of 25 °C. The study of the kinetics of adsorption was carried out by the addition of 1.0 g (±0.01 g) of RM or NRM in 1 mmol 25 mL^{-1} trace metal solution, at pH 5.0–5.5. The samples were stirred at 145 rpm and removed after 15, 30, 60, 120, 420, 660 and 1440 min. The influence of temperature on the adsorption was studied by adsorption tests at different temperatures, i.e. 303 K (30 °C), 313 K (40 °C) and 323 K (50 °C), using 1.00 g (±0.01 g) of RM or NRM in 1 mmol 25 mL^{-1} trace metal solution, at pH 5.0–5.5, with the samples stirred at 145 rpm, for 7 h.

After each experiment, an aliquot was collected from the supernatant and was centrifuged for 25 min at 3000 rpm for analysis of the remaining metal concentration. The trace metals concentrations were determined by inductively coupled plasma optical emission spectrometry (ICP OES), iCAP 6000 SERIES machine Thermo Scientific, with the detection limits of 0.002, 0.006 and 0.001 mg L^{-1} for Ni(II), Pb(II) and Zn(II), respectively, at Center for Environmental Studies—UNESP, Rio Claro. Deionised water was used as a blank sample. All experiments were performed in triplicate. The amount of metal adsorbed onto the RM and NRM, q_e, in mmol g^{-1}, was calculated using Eq. 11. The Eq. 12 was used to obtain the adsorption percentage (%*A*) of metals.

$$q_e = \frac{C_0 - C_e}{m} \cdot V \tag{11}$$

$$\%A = \frac{C_0 - C_e}{C_e} .100 \tag{12}$$

where

C_0 and C_e = initial and equilibrium concentration of metal, respectively, (mmol 25 mL^{-1}); m = mass of adsorbent sample (1 g); V = volume of solution (25 mL).

4 Results and Discussion

4.1 Characterisation of RM and NRM

Properties of RM and NRM are provided in Table 1. Natural red mud possesses alkaline pH and presents the EC value of 3800 μS cm^{-1}. After the neutralisation process by $Ca(NO_3)_2$, pH and EC values decrease. CEC values found were practically identical to RM and NRM. Specific surface area (S_{BET}) obtained for NRM is higher than value found for RM. Pore sizes of RM and NRM ranging from 3.0 to 4.5, indicating the dimensions of mesopores. RM and NRM are composed of particles of different size, shape and texture (Fig. 1), since red mud is a heterogeneous material with particles ranging from <1 to >10 μm of diameter. The mineral morphology was not changed after the $Ca(NO_3)_2$ activation.

Red mud composition is extremely dependent on the bauxite ore origin and the applied technological process,

Table 1 Characterisation of RM and NRM

Parameter	RM	NRM
pH	10.4	7.8
EC (μS cm^{-1})	3800	122
CEC ($mmol_{(+)}$ kg^{-1})	108	110
S_{BET} (m^2 g^{-1})	31.25	40.07
Pores size (nm)	3 to 4	3.5 to 4.5

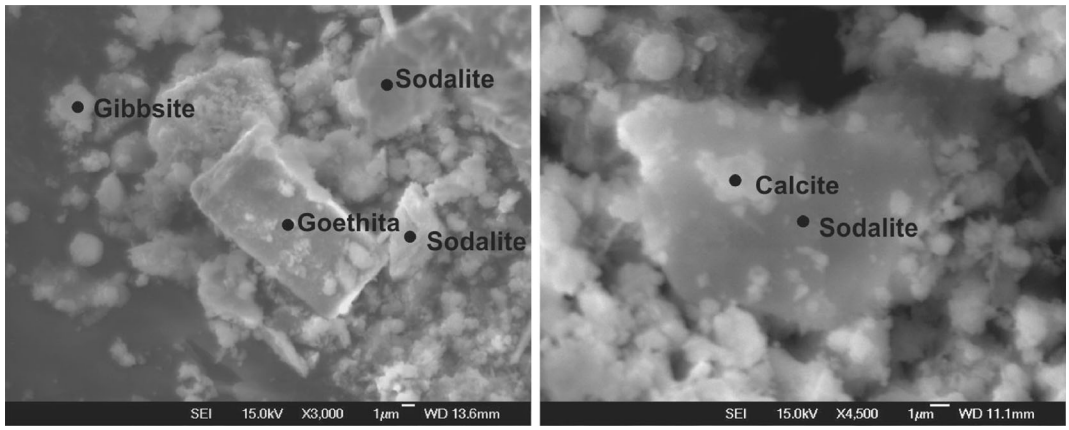

Fig. 1 SEM-EDS of RM (**a**) and NRM (**b**)

and may have different ratios of oxides in other locations (Antunes et al. 2012). Chemical composition of RM and NRM are shown in Table 2. Principal components in both materials are iron, aluminium and silicon oxides. However, the results indicated that the NRM exhibits more calcium oxide than RM. X-Ray diffraction (XRD) patterns of RM and NRM are given in Fig. 2. RM is composed of gibbsite ($Al(OH)_3$), kaolinite ($Al_2Si_2O_5(OH)_4$), quartz (SiO_2), goethite (FeO(OH)), hematite (Fe_2O_3) and sodalite ($Na_8Al_6Si_6O_{24}Cl_2$). NRM possesses the same mineral phases and calcite ($CaCO_3$), which appearing in several peaks in XRD patterns.

The characterisation results of RM and NRM clearly indicate that red mud pH was neutralised, besides EC has decreased (Table 1). EC value reduction occurred due to solubilisation of cations adsorbed in RM during $Ca(NO_3)_2$-neutralisation, because $Ca(NO_3)_2$ has extracted the exchangeable phases of red mud (Santona et al. 2006; Costa et al. 2009), especially those cations that are adsorbed in sodalite mineral phase, such as aluminium, silicon and sodium, amongst others. Several studies have evaluated the neutralisation of red mud with seawater, which concluded that reduction of pH values is associated with reactions between the carbonate and bicarbonate alkalinity of red mud and calcium to form calcite ($CaCO_3$) (McConchie et al. 2000; Hanahan et al. 2004). These studies were carried out to evaluate the adsorption capacity of cadmium (Grudić et al. 2013), arsenate, vanadate and molybdate (Palmer et al. 2010). Recently, Souza et al. (2013a) explained the influence of the thermal treatment of seawater neutralised red mud on the adsorption of Reactive Blue 19 dye.

Table 2 Chemical composition (wt%) of RM and NRM

Oxide	RM	NRM
SiO_2	16.29	14.85
TiO_2	8.66	8.72
Al_2O_3	17.50	16.49
Fe_2O_3	35.77	35.06
MnO	0.24	0.27
MgO	0.10	0.12
CaO	3.55	8.19
Na_2O	4.45	3.31
K_2O	0.37	0.29
P_2O_5	0.37	0.39
LOI	12.60	12.32
Total	99.90	100.01

During the activation, the $Ca(NO_3)_2$ is dissolved in water solution ($Ca(NO_3)_2 \rightarrow Ca^{2+} + (NO_3)_2{}^{2-}$) and the Ca^{2+} reacts with alkalinity from red mud to precipitate calcite, according to Eqs. 13 and 14. XRD and MEV-EDS analysis confirmed the presence of calcite in NRM (Figs. 1 and 2). Besides, the chemical composition of NRM also indicates an increase in Ca^{2+} content in relation to RM due to calcite formation during $Ca(NO_3)_2$-neutralisation (Table 2). The increase in S_{BET} value can also be explained by the formation of calcite in the surface of red mud grains (Fig. 1b).

$$OH^-_{(aq)} + CO_{2(aq)} \rightarrow HCO_3{}^-_{(aq)} \quad (13)$$

$$2HCO_3{}^-_{(aq)} + Ca^{2+}_{(aq)} \rightarrow CaCO_3(s) + H_2CO_{3(aq)} \quad (14)$$

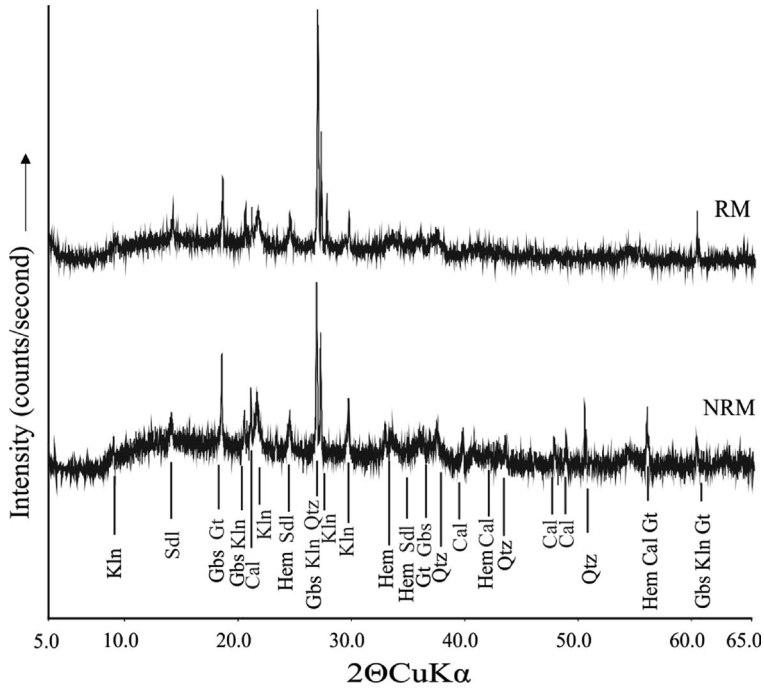

Fig. 2 XRD patterns of RM and NRM. *Sodalite* Sdl, *Gibbsite* Gbs, *Goethite* Gt, *Kaolinite* Kln, *Hematite* Hem, *Quartz* Qtz and *Calcite* Cal

4.2 Influence of pH in Adsorption Experiments

The removal of Ni(II), Pb(II) and Zn(II) by RM and NRM at different values of pH is given in Fig. 3. In the experiments at pH 10 and 12, values of C_0 e C_e were lower than metal limit detection of ICP OES device, propably due to precipitation of these metals, as indicated in the literature (Bhattacharyya and Gupta 2008; Zhou and Haynes 2011). This precipitation was confirmed using the software CHEAQS (CHemical Equilibria in Aquatic Systems) (Verweij 2014), which function is to calculate the chemical equilibrium in aqueous systems and find the chemical speciation of chemical compounds. Thus, the results obtained in experiments performed at pH 10 and 12 were not considered, because this study had interest to investigate adsorption of dissolved metals in aqueous solution.

For all metals, the removal efficiency increases at pH 7. The removal efficiency was practically equal for the RM and NRM in all pH values considering the associated standard deviation. Thus, the $Ca(NO_3)_2$ neutralisation process does not affect the removal efficiency of Ni(II), Pb(II) and Zn(II) in aqueous solution. For the concentration tested, at pH 7 the highest values of

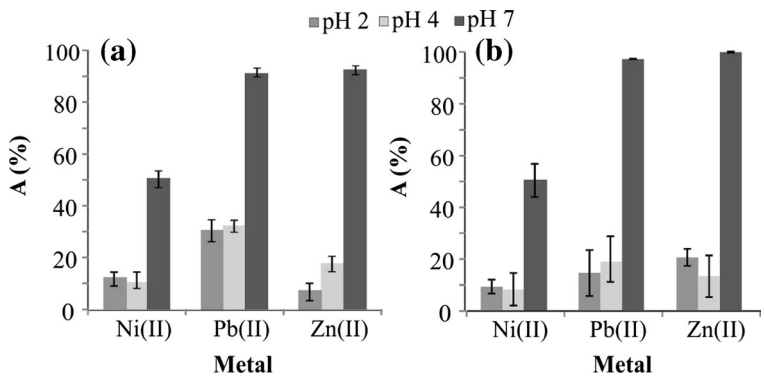

Fig. 3 Effect of pH on the adsorption of Ni(II), Pb(II) and Zn(II) by RM (**a**) and NRM (**b**) in different pH conditions. *Bars* indicate standard deviation

percentages removal were 53% for Ni(II) in RM, 97% for Pb(II) in NRM and 99% for Zn(II) in NRM. In highly acidified solution, at pH 2 and 4, the highest removal efficiency was ca. 30%, indicating a weak adsorption process in relation to solution at pH 7.

Although the value of 7 has been found as the optimum pH, the initial pH of RM and NRM samples with metals in aqueous solutions varied between 5.0 and 5.5, which is a value widely used in adsorption studies (Santona et al. 2006; Nadaroglu et al. 2010; Smiljanic et al. 2010; Smiciklas et al. 2014). This value is considered ideal because at acid pH, metals precipitation does not occur, and pH is not so low, which could adversely affect the adsorption. In addition, when carrying up the other adsorption experiments at natural pH of the medium, studies are more practical and economical because it is not necessary pH adjustment and use of acidic and basic reagents.

4.3 Adsorption Isotherms

The total amount of Ni(II), Pb(II) and Zn(II) in the aqueous solutions was higher than the cationic exchange capacity of RM and NRM. The removal of these metals by RM and NRM was higher than their respective CEC. Figure 4 shows adsorption isotherms adjusted by Freundlich and Langmuir models for the Ni(II), Pb(II) and Zn(II) onto RM and NRM. Freundlich and Langmuir isotherm's parameters are shown in Table 3. For all samples, the relative standard deviation was lower than 4%.

Metal adsorption on RM and NRM was practically identical and increased in the following order: $Zn(II) \leq Ni(II) < Pb(II)$ (mmol g^{-1}) (Fig. 4). Ni(II), Pb(II) and Zn(II) adsorption was higher than 68% at lower concentrations (0.5 to 1.0 mmol 25 mL^{-1}). When the Ni(II), Pb(II) and Zn(II) concentrations increase, the adsorption in RM and NRM decreases, indicating that the efficiency of adsorption is lower for the highest concentrations. The highest values of R^2 were obtained for Freundlich model for both materials, as well as this model tends to better represent the average of experimental, considering the *ARE* values (Table 3). Thus, for this application, the Freundlich model represents the phenomenon of adsorption of Ni(II), Pb(II) and Zn(II) on RM and NRM.

The maximum adsorption capacity values (q_{max}) of RM and NRM were 1.78 and 1.79 mmol g^{-1} for Ni(II), 2.13 and 2.23 mmol g^{-1} for Pb(II) and 1.14 and 1.06 mmol g^{-1} for Zn(II), at pH 5.0–5.5, respectively. The values of RM and NRM adsorption capacity of Ni(II) and Pb(II) (in mmol g^{-1}) were higher than the values obtained in the literature to natural or activated red mud (Table 4) (Apak et al. 1998b; Gupta et al. 2001; Santona et al. 2006; Hannachi et al. 2010; Smiljanic et al. 2010;

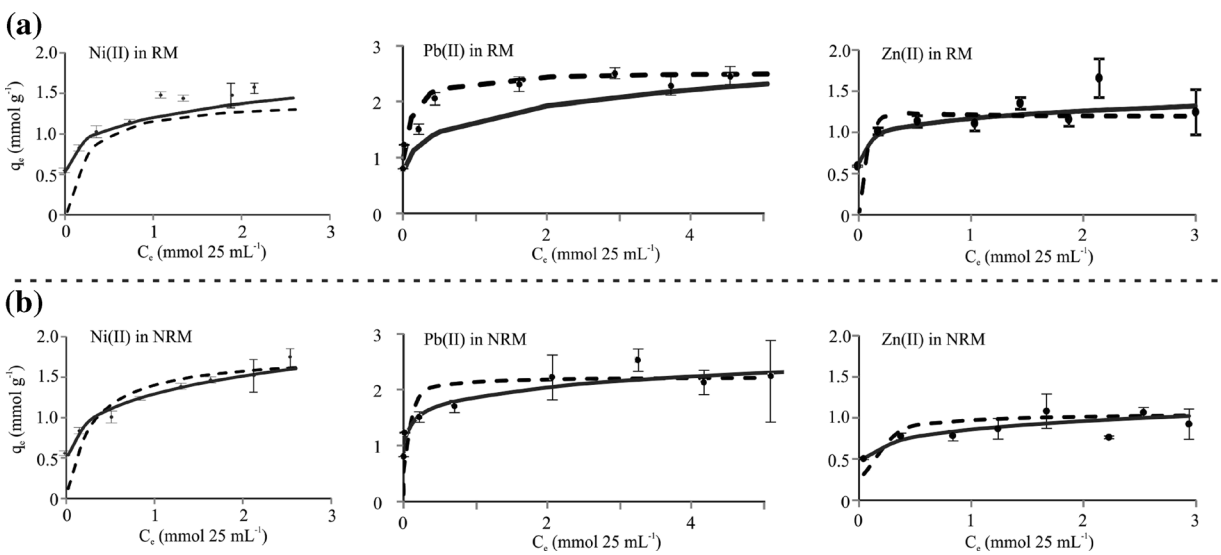

Fig. 4 Adsorption isotherms of Ni(II), Pb(II) and Zn(II) by RM and NRM (**a** and **b**, respectively) using Langmuir (*continuous line*) and Freundlich (*dashed line*) adsorption models. *Bars* indicate standard deviation

Table 3 Parameter of adsorption using Freundlich and Langmuir models for Ni(II), Pb(II) and Zn(II) adsorption by RM and NRM, at pH 5–5.5

	Freundlich parameters				Langmuir parameters			
	K_F ((mmol g^{-1}) (25 mL $mmol^{-1})^{1/n}$)	*1/n*	R^2	ARE	q_{max} (mmol g^{-1})	K_L (25 mL $mmol^{-1}$)	R^2	ARE
RM								
Ni(II)	1.36	0.21	0.99	0.69	1.78	4.56	0.97	8.11
Pb(II)	1.68	0.20	0.99	0.58	2.13	11.37	0.99	1.37
Zn(II)	1.12	0.12	0.99	−0.59	1.14	−46.76	0.96	11.72
NRM								
Ni(II)	1.29	0.23	0.96	−0.27	1.79	3.57	0.97	6.59
Pb(II)	1.88	0.13	0.99	0.34	2.23	23.9	0.99	10.59
Zn(II)	0.86	0.16	0.99	−0.65	1.06	10.34	0.92	−2.69

Pulford et al. 2012; Smiciklas et al. 2014). For Zn(II), adsorption capacity was lower than the natural red mud (Vaclavikova et al. 2005; Santona et al. 2006) and treated by HCl (Santona et al. 2006) and higher than the red mud neutralised by CO_2 (Sahu et al. 2011), treated by $CaSO_4$ (Lopez et al. 1998) and thermally treated (Gupta and Sharma 2002) (Table 4).

Sodalite (calcium and sodium tectosilicate) possesses open porous structure, being found in RM and NRM.

Table 4 Comparison of RM and NRM adsorption capacity (mmol g^{-1}) with other studies

Metal	Treatment	Adsorption capacity	Reference
Ni(II)	RM—natural	1.78	Present study
	NRM—$Ca(NO_3)_2$	1.79	Present study
	Natural red mud	0.23	Hannachi et al. (2010)
	Red mud—HCl	0.19	Smiciklas et al. (2014)
	Red mud—thermal	0.37	Smiljanic et al. (2010)
Pb(II)	RM—natural	2.13	Present study
	NRM—$Ca(NO_3)_2$	2.23	Present study
	Natural red mud	1.88	Santona et al. (2006)
	Red mud—carbonised	0.45	Pulford et al. (2012)
	Red mud—HCl	0.84	Apak et al. (1998b)
	Red mud—HCl	0.77	Santona et al. (2006)
	Red mud—thermal and H_2O_2	0.35	Gupta et al. (2001)
Zn(II)	RM—natural	1.14	Present study
	NRM—$Ca(NO_3)_2$	0.96	Present study
	Natural red mud	2.05	Vaclavikova et al. (2005)
	Natural red mud	2.47	Santona et al. (2006)
	Red mud—$CaSO_4$	0.19	Lopez et al. (1998)
	Red mud—CO_2	0.23	Sahu et al. (2011)
	Red mud—HCl	1.59	Santona et al. (2006)
	Red mud—thermal	0.18-0.22	Gupta and Sharma (2002)

This mineral is considered as zeolite-type mineral and exhibits permanently negatively-charged surface (Smiciklas et al. 2014), which is responsible for the adsorption capacity of RM and NRM. Besides, other minerals (Al and Fe oxides) also allows the adsorption of Ni(II), Pb(II) and Zn(II) (Santona et al. 2006), which were found in RM and NRM (Fig. 2).

4.4 Kinetic Studies

The adsorption kinetics of Ni(II), Pb(II) and Zn(II) by RM and NRM, at pH 5.0–5.5 are shown in Figure 5. It can be seen that the stabilisation of adsorption has started from 420 min for all metals. This time of 7 h was considered as minimum time for adsorption tests.

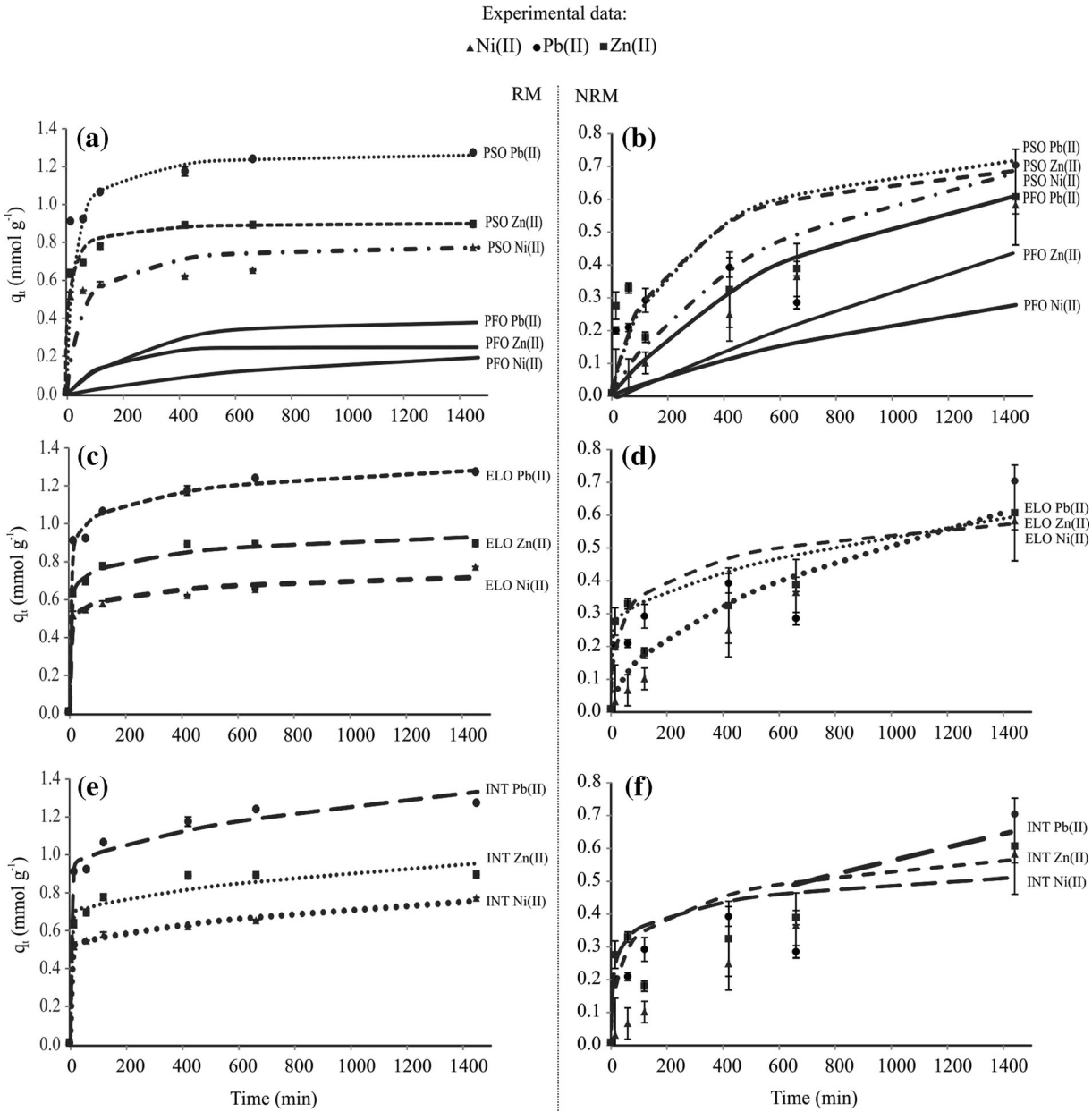

Fig. 5 q_t versus adsorption time of Ni(II), Pb(II) and Zn(II) using RM and NRM adjusted by pseudo-first-order Lagergren—PFO, pseudo-second-order—PSO, Elovich—ELO and intraparticle diffusion—INT models (**a**, **b**, **c**, **d**, **e** and **f**, respectively). *Bars* indicate standard deviation

The parameters shown in Table 5 were obtained from the adjustment of the kinetic models to the adsorption experimental data, at pH 5.0–5.5, using pseudo-first order Lagergren (Fig. 5a, b), pseudo-second order (Fig. 5a, b), Elovich (Fig. 5c, d) and intraparticle diffusion (Fig. 5e, f) models.

Comparing the parameters of the pseudo-first-order Lagergren and pseudo-second-order models, and their adjustment to the experimental data based on the *ARE* values and R^2 (Table 5), it is clear that *ARE* values are lower for the model of pseudo-second order, for all metals, for RM and NRM. The R^2 values obtained to pseudo-second order were higher than values found for pseudo-first Lagergren model (except for Ni(II) adsorption on NRM). For the pseudo-second-order model, q_e values are closer to the values of $q_{e(exp)}$, except for the Ni(II) adsorption on NRM. Besides, according to the *ARE* and R^2 values, the pseudo-second-order model indicated the best fit to the experimental data for all metals by RM and NRM.

The absolute values of *ARE* for Elovich and intraparticle diffusion models can be considered low, except for the Ni(II) and Zn(II) adsorption on NRM. The R^2 varied from 0.48 to 0.95 for Elovich model and from 0.73 to 0.99 for intraparticle diffusion model. The intercept values presents in Table 5 suggest that the surface adsorption and intraparticle-diffusion were only concurrently occurring during the adsorption of Ni(II), Pb(II) and Zn(II) on RM and NRM.

4.5 Thermodynamic Studies

The percentage of adsorption of Ni(II), Pb(II) and Zn(II) by RM and NRM at different temperatures (303, 313 and 323 K), at pH 5.0–5.5, is given in Fig. 6a, b, respectively. The percentage adsorption of these metals increases with increasing temperature. The constants $\Delta H°$ and $\Delta S°$ were obtained from the slope and intercept of plot $ln\ K_c$ versus $T^{-1}10^3$ (van't Hoff chart) (Fig. 6c, d), respectively. Table 6 presents the thermodynamic parameters obtained, $\Delta H°$ (kJ mol^{-1}), $\Delta S°$ (J (mol K)$^{-1}$) and $\Delta G°$ (kJ mol^{-1}). Positive values for $\Delta H°$ indicated the occurrence of endothermic reactions and positive values of $\Delta S°$ indicated affinity of the RM

Table 5 Kinetic parameters obtained by pseudo-first order, pseudo-second order, Elovich and intraparticle diffusion models for Ni(II), Pb(II) and Zn(II) adsorption by RM and NRM, at pH 5–5.5

$q_{e(exp)}$ (mmol g^{-1})	RM			NRM		
	Ni(II) 0.77	Pb(II) 1.28	Zn(II) 0.90	Ni(II) 0.58	Pb(II) 0.71	Zn(II) 0.61
Pseudo-first order						
q_e (mmol g^{-1})	0.24	0.39	0.26	0.57	0.47	0.35
$k_1 \times 10^3$ (min^{-1})	1.15	3.70	7.13	1.38	0.46	0.69
R^2	0.97	0.98	0.92	0.99	0.33	0.51
ARE	88.54	0.82	79.94	22.11	0.81	80.81
Pseudo-second order						
q_e (mmol g^{-1})	0.78	1.20	0.90	0.81	0.68	0.63
$k_2 \times 10^3$ (g (mmol min)$^{-1}$)	25.42	33.81	88.16	1.75	6.01	7.67
R^2	0.99	0.99	0.99	0.87	0.71	0.90
ARE	12.73	0.06	1.87	1.66	0.13	11.32
Elovich						
α (mmol (g min)$^{-1}$)	59.87	95.25	76.75	0.0046	0.03	0.12
β (g mmol^{-1})	19.96	11.09	15.41	8.67	11.52	17.01
R^2	0.86	0.95	0.94	0.84	0.61	0.48
ARE	−0.16	0.001	−0.14	22.78	0.05	−8.29
Intraparticle diffusion						
k_{int} (mmol (g min^{½})$^{-1}$)	0.0071	0.01	0.0078	0.0165	0.013	0.0096
C	0.49	0.89	0.66	−0.06	0.12	0.18
R^2	0.98	0.88	0.78	0.99	0.78	0.73
ARE	0.15	0.002	−0.42	9.74	0.03	−5.24

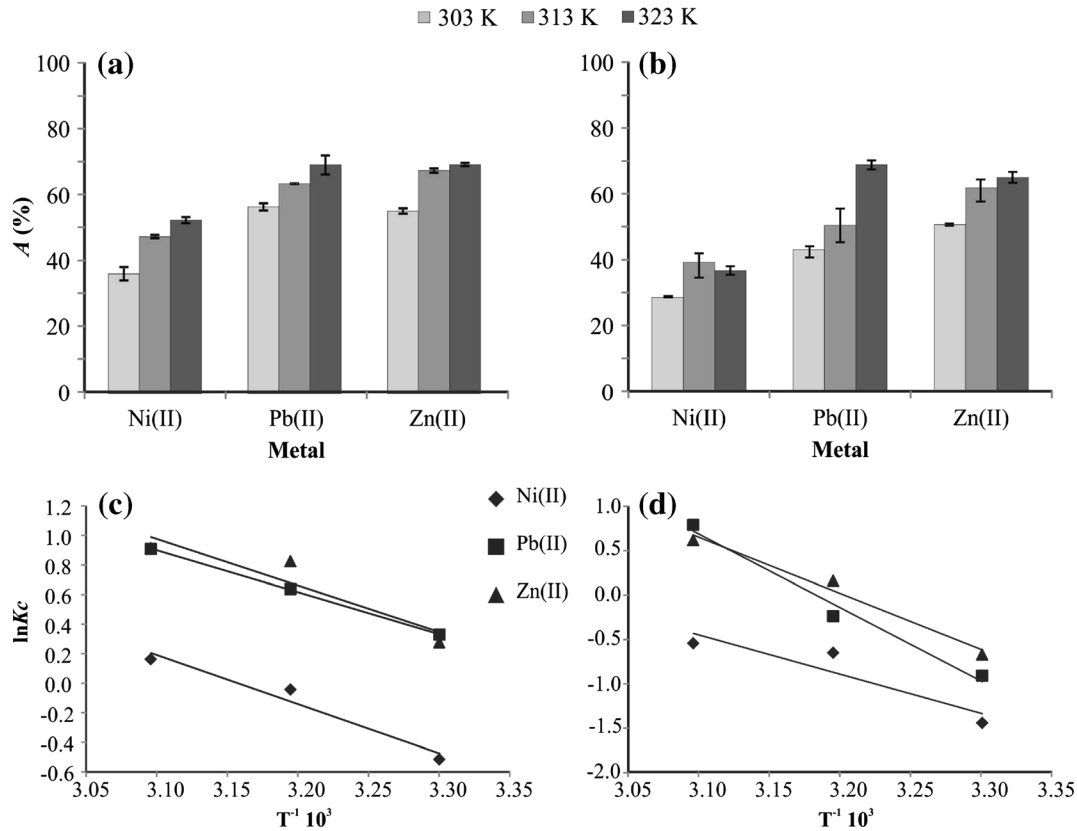

Fig. 6 Adsorption of Ni(II), Pb(II) and Zn(II) by RM and NRM at different temperatures (303, 313 and 323 K) and van't Hoff chart ($\ln K_c$ versus $T^{-1}10^3$) for Ni(II), Pb(II) and Zn(II) by RM and NRM (**a**, **b**, **c** and **d**, respectively). *Bars* indicate standard deviation

and NRM for Ni(II), Pb(II) and Zn(II) (Chowdhury et al. 2011). For $\Delta G°$, negative and positive values were observed. Negative values confirmed the natural spontaneity of the adsorption process, which is the case at 303 K for Pb(II) and Zn(II) adsorption on RM, at 313 K for Pb(II) adsorption on RM and Zn(II) adsorption on RM and NRM and at 323 K for all cases, except for Ni(II) adsorption on NRM. The growth of the absolute value of $\Delta G°$ with increasing temperature suggests an increase in adsorption affinity of Ni(II), Pb(II) and Zn(II) for RM and NRM with temperature (Chowdhury et al. 2011).

Table 6 Thermodynamic parameters obtained for Ni(II), Pb(II) and Zn(II) adsorption by RM and NRM, at pH 5–5.5

	$\Delta H°$ (kJ mol^{-1})	$\Delta S°$ (J (mol K)$^{-1}$)	$\Delta G°$ (kJ mol^{-1})		
		RM	303 K	313 K	323 K
Ni(II)	27.69	87.27	1.30	1.13	−0.44
Pb(II)	23.54	80.46	−0.83	−1.66	−2.44
Zn(II)	26.17	89.24	−0.69	−2.15	−2.45
NRM					
Ni(II)	36.86	110.54	3.63	1.69	1.46
Pb(II)	68.95	219.46	2.29	0.62	−2.12
Zn(II)	52.58	168.40	1.69	−0.42	−1.66

5 Conclusion

The chemical treatment with $Ca(NO_3)_2$ has caused pH neutralisation of the red mud, which is a very important factor for the reuse of this waste of bauxite refining. This occurs due to reactions between the carbonate and bicarbonate alkalinity of red mud and calcium from calcium nitrate to form calcite ($CaCO_3$), fact confirmed with the chemical and mineralogical results of RM and NRM. The adsorption of Ni(II), Pb(II) and Zn(II) on RM and NRM was dependent on the pH of the solution, with the highest percentage of adsorption occurs at pH 7. The adsorption isotherm model that best represented the adsorption of these metals on RM and NRM was the Freundlich model. The q_{max} values of RM and NRM, respectively, were 1.78 and 1.79 mmol g^{-1} for Ni(II), 2.13 and 2.23 mmol g^{-1} for Pb(II), and 1.14 and 1.06 mmol g^{-1} for Zn(II), respectively. Sodalite is responsible for the adsorption capacity of RM and NRM. The pseudo-second kinetic order model presented the best fit to the experimental data for these metals. The percentage of adsorbed metal increased with increasing temperature and the values of $\Delta H°$ and $\Delta S°$ were positive, indicating that the adsorption reaction is endothermic and affinity between these metals and RM and NRM. Thus, this study presents an important alternative to neutralised the red mud, which can be used for the treatment of water and wastewaters with the same efficient of RM.

Acknowledgements The authors acknowledge the Fundação de Amparo à Pesquisa do Estado de São Paulo (FAPESP—Processes No. 2009/02374-0 and 2013/00994-6), Conselho Nacional de Desenvolvimento Científico e Tecnológico (CNPq—Process No. 480555/2009-5) and Companhia Brasileira de Alumínio (CBA).

References

Akin, I., Arslan, G., Tor, A., Ersoz, M., & Cengeloglu, Y. (2012). Arsenic (V) removal from underground water by magnetic nanoparticles synthesized from waste red mud. *Journal of Hazardous Materials, 235–236*, 62–68.

Antunes, M. L. P., Couperthwaite, S. J., Conceição, F. T., Jesus, C. P. C., Kiyohara, P. K., Coelho, A. C. V., & Frost, R. L. (2012). Red mud from Brazil: thermal behavior and physical properties. *Industrial and Engineering Chemistry Research, 51*, 775–779.

Apak, R., Guclu, K., & Turgut, M. H. (1998a). Modeling of copper (II), cadmium (II) and lead (II) adsorption on red mud. *Journal of Colloid and Interface Science, 203*, 122–130.

Apak, R., Tütem, E., Hügül, M., & Hizal, J. (1998b). Heavy metal cation retention by unconventional sorbents (red muds and fly ashes). *Water Research, 32*, 430–440.

Behnamfard, A., Salarirad, M. M., & Vegliò, F. (2014). Removal of Zn(II) ions from aqueous solutions by ethyl xanthate impregnated activated carbons. *Hydrometallurgy, 144–145*, 39–53.

Bhattacharyya, K. G., & Gupta, S. S. (2008). Influence of acid activation on adsorption of Ni(II) and Cu(II) on kaolinite and montmorillonite: kinetic and thermodynamic study. *Chemical Engineering Journal, 136*, 1–13.

Brasil. Departamento Nacional de Produção Mineral, Lima, T.M., Neves, C.A.R. (Coord.) (2014). Sumário Mineral, DNPM, Brasília.

Cengeloglu, Y., Tor, A., Ersoz, M., & Turgut, M. H. (2006). Removal of nitrate from aqueous solution by using red mud. *Separation and Purification Technology, 51*, 374–378.

Cheung, C. W., Porter, J. F., & Mckay, G. (2000). Sorption kinetics for the removal of cooper and zinc from effluents using bone char. *Separation and Purification Technology, 19*, 55–64.

Chowdhury, S., Mishra, R., Saha, P., & Kushwaha, P. (2011). Adsorption thermodynamics, kinetics and isosteric heat of adsorption of malachite green onto chemically modified rice husk. *Desalination, 265*, 159–168.

Conceição, F. T., Pichinelli, B. C., Silva, M. S. G., Moruzzi, R. B., Menegário, A. A., & Antunes, M. L. P. (2016). Cu(II) adsorption from aqueous solution using red mud activated by chemical and thermal treatment. *Environmental Earth Sciences, 75*, 362.

Costa, E. T. S., Guilherme, L. R. G., Curi, N., Lopes, G., Visoli, E. L., & Oliveira, L. C. A. (2009). Caracterização de subproduto da indústria de alumínio e seu uso na retenção de cádmio e chumbo em sistemas monoelementares. *Química Nova, 32*, 868–847.

Di Bernardo, L. (2005). Métodos e técnicas de tratamento de água, 2 V, RiMA, São Carlos.

Embrapa (1997). Manual de Métodos de Análise de Solo, 2° ed., Centro Nacional de Pesquisa de Solos, Rio de Janeiro.

Fu, J., Song, R., Mao, W., Wang, Q., An, S., Zeng, Q., & Zhua, H. (2010). Adsorption of disperse blue 2BLN by microwave activated red mud. *Environmental Progress & Sustainable Energy, 30*, 558–566.

Geyikçi, F., Kiliç, E., Çoruh, S., & Elevli, S. (2012). Modeling of lead adsorption from industrial sludge leachate on red mud by using RSM and ANN. *Chemical Engineering Journal, 183*, 53–59.

Grudić, V. V., Brašanac, S., Vukašinović-Pešić, V. L., & Blagojević, N. Z. (2013). Sorption of cadmium from water using neutralized red mud and activated neutralized red mud. *ARPN Journal of Engineering and Applied Science, 8*, 933–943.

Gupta, V. K., Gupta, M., & Sharma, S. (2001). Process development for the removal of lead and chromium from aqueous solutions using red mud—an aluminum industry waste. *Water Research, 35*, 1125–1134.

Gupta, V. K., & Sharma, S. (2002). Removal of cadmium and zinc from aqueous solutions using red mud. *Environmental Science and Technology, 36*, 3612–3617.

Hanahan, C., McConchie, D., Pohl, J., Creelman, R., Clark, M., & Stocksiek, C. (2004). Chemistry of seawater neutralization of bauxite refinery residues (Red Mud). *Environmental Engineering Science, 21*, 125–138.

Hannachi, Y., Shapovalov, N. A., & Hannachi, A. (2010). Adsorption of Nickel from aqueous solution by the use of low-cost adsorbents. *Korean Journal of Chemical Engineering, 27*(1), 152–158.

Hind, A. R., Bhargava, S. K., & Grocott, S. C. (1999). The surface chemistry of Bayer process solids: a review. *Colloids and Surfaces A, 146*, 359–374.

Ho, Y. S., & Mckay, G. (1998). A comparison of chemisorption kinetic models applied to pollutant removal on various sorbents. *Transactions of the Institution of Chemical Engineers, 76*, 332–340.

Liang, W., Couperthwaite, S. J., Kaur, G., Yan, C., Jonhstone, D. W., & Millar, G. I. J. (2014). Effect of strong acids on red mud structural and fluoride adsorption properties. *Journal of Colloid and Interface Science, 423*, 158–165.

Lopez, E., Soto, B., Arias, M., Nunez, A., Rubinos, D., & Barral, M. T. (1998). Adsorbent properties of red mud and its use for wastewater treatment. *Water Research, 32*, 1314–1322.

Mártires, R.A.C. (2012). Alumínio, in: Brasil. Departamento Nacional de Produção Mineral. Lima, T.M., Neves, C.A.R. (Coord.), Sumário Mineral, DNPM/DIPLAM, Brasília.

McConchie, D., Clark, M., Hanahan, C., McConchie, F. (2000). The use of seawater-neutralised bauxite refinery residues in the management of acid sulphate soils, sulphidric mini tailings and acid mine drainage. In K. Gaul, Ed., 3rd Queensland Environmental Conference: Sustainable Solutions for Industry and Government. Brisbane, QLD, Australia, 201–208.

Nadaroglu, H., Kalkan, E., & Demir, N. (2010). Removal of copper from aqueous solution using red mud. *Desalination, 251*, 90–95.

Önal, Y. (2006). Kinetics of adsorption of dyes from aqueous solution using activated carbon prepared from waste apricot. *Journal of Hazardous Materials B, 137*, 1719–1728.

Palmer, S. J., Nothling, M., Bakon, K. H., & Frost, R. L. (2010). Thermally activated seawater neutralised red mud used for removal of arsenate, vanadate and molybdate from aqueous solutions. *Journal of Colloid and Interface Science, 342*, 147–154.

Pulford, I. D., Hargreaves, J. S. J., Durisová, J., Kramulova, B., Girard, C., Balakrishnan, M., Batra, V. S., & Rico, J. L. (2012). Carbonised red mud—a new water treatment product made from a waste material. *Journal of Environmental Management, 100*, 59–64.

Rai, S., Wasewar, K. L., Mukhopadhyay, J., Yoo, C. K., & Uslu, H. (2012). Neutralization and utilization of red mud for its better waste management. *Archives of Environmental Science, 6*, 13–33.

Ratnamala, G. M., Vidya Shetty, K., & Srinikethan, G. (2012). Removal of remazol brilliant blue dye from dye-contaminated water by adsorption using red mud: equilibrium, kinetic and thermodynamic studies. *Water, Air, and Soil Pollution, 223*, 6187–6199.

Sahu, R. C., Patel, R., & Ray, B. C. (2011). Adsorption of Zn(II) on activated red mud: neutralized by CO_2. *Desalination, 266*, 93–97.

Santana, A. L. (2014). Alumínio, in: Brasil. Departamento Nacional de Produção Mineral. Lima, T.M., Neves, C.A.R. (Coord.), Sumário Mineral, DNPM, Brasília.

Santona, L., Castaldi, P., & Melis, P. (2006). Evaluation of the interaction mechanisms between red mud and heavy metals. *Journal of Hazardous Materials, 136*, 324–329.

Silva Filho, E. B., Alves, M. C. M., & Motta, M. (2007). Lama vermelha da indústria de beneficiamento de alumina: produção, características, disposição e aplicações alternativas. *Revista Matéria, 12*, 322–338.

Smiciklas, I., Smiljanic, S., Peric-Grujic, A., Šljivic-Ivanovic, M., Mitric, M., & Antonovic, D. (2014). Effect of acid treatment on red mud properties with implications on Ni(II) sorption and stability. *Chemical Engineering Journal, 242*, 27–35.

Smiljanic, S., Smiciklas, I., Peric-Grujic, A., Loncar, B., & Mitri, M. (2010). Rinsed and thermally treated red mud sorbents for aqueous Ni^{2+} ions. *Chemical Engineering Journal, 162*, 75–83.

Souza, K. C., Antunes, M. L. P., Couperthwaite, S. J., Conceição, F. T., Barrs, T. R., & Frost, R. (2013a). Adsorption of reactive dye on seawater-neutralised bauxite refinery residue. *Journal of Colloid and Interface Science, 396*, 210–214.

Souza, K. C., Antunes, M. L. P., & Conceição, F. T. (2013b). Adsorção do corante reativo azul 19 em solução aquosa por lama vermelha tratada quimicamente com peróxido de hidrogênio. *Quim Nova, 36*, 651–656.

Tchobanoglous, G., Burton, F.L., Stensel, H.D., 2003. Wastewater engineering: Treatment and reuse, fourth ed., Metcalf & Eddy, Inc., McGraw-Hill, Boston.

Vaclavikova, M., Misaelides, P., Gallios, G., Jakabsky, S., & Hredzak, S. (2005). Removal of cadmium, zinc, copper and lead by red mud, an iron oxides containing hydrometallurgical waste. *Studies in Surface Science and Catalysis, 155*, 517–525.

Verweij, W., (2014). A program for calculating CHemical Equilibria in AQuatic Systems, CHEAQS PRO 2014.1, Netherlands, 1999–2014.

Wang, S., Ang, H. M., & Tadé, M. O. (2008). Novel applications of red mud as coagulant, adsorbent and catalyst for environmentally benign processes. *Chemosphere, 72*(3), 1621–1635.

Zhou, Y., & Haynes, R. J. (2011). A comparison of inorganic solid wastes as adsorbents of heavy metal cations in aqueous solution and their capacity for desorption and regeneration. *Water, Air, and Soil Pollution, 218*, 457–470.